15TH IEA HEAT PUMP CONFERENCE
MAY 26–29, 2026 | HOFBURG
VIENNA 2026
DECARBONISATION THROUGH INNOVATION

Optimal Design of an Industrial Steam Heat Pump for the Paper Drying Process

Kijeong Seo[a], Minkyu Jung[a], Hyunmin Yang[b], Yeontae Jeong[b], Ho-Seong Lee[c], Minsung Kim[a,b,*]

[a]Department of Intelligent Energy and Industry, Chung-Ang University, 84 Heukseok-ro, Dongjak-gu, Seoul 06974, Republic of Korea
[b]Department of Energy Systems Engineering, Chung-Ang University, 84 Heukseok-ro, Dongjak-gu, Seoul 06974, Republic of Korea
[c]Integrated Thermal Management System R&D Center, Korea Automotive Technology Institute (KATECH), 303 Pungse-ro, Pungse-myeon, Cheonan-si, Chungcheongnam-do 31214, Republic of Korea

Abstract

Steam, owing to its rapid and stable heat transfer characteristics through latent heat, is widely used in various drying industries such as food, biomass, chemical, laundry, and pulp and paper. As the electrification of industrial steam generation replaces fossil fuels like coal and natural gas, steam heat pumps have gained attention as a key technology for realizing low-carbon and high-efficiency steam production. By utilizing low-grade waste heat from manufacturing processes to regenerate high-temperature steam, steam heat pumps offer higher efficiency and lower carbon emissions compared to conventional boilers. For practical application, however, detailed quantification of waste-heat conditions, including temperature and mass flow rate, is essential to design appropriate system capacity and operating conditions. In this study, the paper-drying process was analyzed using factory energy management system (F-EMS) data, and performance sweeps were conducted by varying the evaporator air-side approach temperature (ΔT). The results indicated optimal ΔT* values ranging from 15 to 25 °C, achieving the highest cost efficiency at a steam production rate of 1.34 kg/s and power consumption of 1.26 MW. When comparing two integration strategies-direct supply to the main header (Scenario 1) and intermediate-pressure supply (Scenario 2)-the latter showed an annual economic advantage of approximately 1.47 MUSD. The system employed a low-GWP, zero-ODP refrigerant R1233zd(E), which enables 2-phase heat exchange above 130 °C. This study demonstrates the feasibility and economic benefits of industrial steam heat pumps utilizing waste heat, contributing to the advancement of electrification in thermal process industries.

Keywords: Factory energy management system; Energy balance; Steam generation heat pump; Mechanical vapor recompression

1. Introduction

Steam has long served as a key thermal medium in industrial processes due to its high heat-transfer capability and controllable characteristics [1-3]. In particular, the drying section of the paper manufacturing process is one of the most steam-intensive stages, where maintaining a stable high-temperature heat supply directly affects product quality and productivity [4-5]. However, most industrial steam is still generated by fossil-fuel boilers, which leads to low energy efficiency and high carbon emissions. To overcome these limitations, industrial facilities are increasingly pursuing electrification, transitioning toward electricity-based heat supply systems to achieve decarbonization and improve energy utilization [6]. The steam generation heat pump (SGHP) represents a central technology in this transition [7]. It recovers low-grade waste heat released from the process and upgrades it to generate high-temperature steam, thereby reducing both fuel consumption and CO_2 emissions compared with conventional boilers. Owing to this advantage, the SGHP is highly applicable in industries with abundant low-temperature exhaust streams, such as paper, food, chemical, laundry,

* Corresponding author. *E-mail address:* minsungk@cau.ac.kr

and biomass processing, contributing significantly to the realization of carbon neutrality across industrial sectors [8]. Another complementary technology is mechanical vapor recompression (MVR), which reuses process steam by compressing it back to a usable pressure [9]. While the SGHP relies on external low-temperature sources such as exhaust air, the MVR minimizes thermal losses by directly recompressing vapor within the process loop.

The actual performance and economics of these systems, however, depend strongly on the physical characteristics of the available waste heat (temperature level, mass flow rate, and humidity) as well as on the configuration of the steam network, pressure conditions, and operating strategy. Despite this, many previous studies have been limited to simplified single-stream or average analyses, lacking detailed optimization based on real factory data. Consequently, it is essential to establish a framework that uses field-measured operational data to analyze thermal energy flows precisely and to develop integrated operating strategies for SGHP and MVR systems suited to real industrial environments.

In this study, the drying section of a paper manufacturing factory was analyzed using long-term operational data obtained from the factory energy management system (F-EMS). Based on these measurements, the characteristics of waste-heat streams and their energy balances were quantified. The air-side approach temperature (ΔT) at the evaporator was selected as the key parameter to evaluate the SGHP performance, compressor power consumption, steam generation rate, and operating cost. Furthermore, two system configurations were compared-direct supply of regenerated steam to the main header and supply to an intermediate-pressure line-to assess differences in energy recovery efficiency and annual cost reduction. A low-GWP refrigerant, R1233zd(E), capable of stable two-phase heat transfer above 130 ℃, was employed to ensure thermodynamic reliability and environmental compatibility in high-temperature steam generation.

2. Energy balance analysis based F-EMS

2.1. Factory energy management system-based operating data analysis

The factory energy management system (F-EMS) serves as the central data platform for monitoring and analyzing the thermal performance of the paper-drying process [10,11]. It integrates signals from distributed sensors installed throughout the factory, encompassing steam, air, and exhaust lines, as well as electrical and mechanical subsystems. The F-EMS continuously logs temperature, pressure, humidity, and flow rate data at one-minute intervals, while also recording electrical power consumption from major drives such as blowers, pumps, and compressors. These data streams are synchronized and stored in a unified database, allowing cross-comparison between thermal and electrical variables. Fig. 1 shows the overall configuration of the F-EMS and the measurement nodes corresponding to the paper-drying process.

The investigated paper-drying line operates as a continuous process throughout the year, and the F-EMS therefore provides long-term operational data covering a wide range of operating conditions.As shown in Fig. 2(a), the raw time-series data include short-term disturbances and abnormal low-value intervals arising from transient operating events and sensor irregularities. To derive representative operating conditions, non-representative periods were removed through data preprocessing, and the remaining data were filtered to extract steady operating intervals. The refined dataset, illustrated in Fig. 2(b), was then used to determine representative boundary conditions for the subsequent energy balance analysis and system simulations.

The system architecture follows a hierarchical structure consisting of local data acquisition units, a factory-level control server, and a cloud-based analytics platform. Each local node communicates via industrial protocols such as Modbus TCP and OPC-UA, ensuring reliable and time-stamped data transfer. Real-time dashboards provide operators with process temperature trends and energy consumption indicators, while the historical database enables analysis of long-term operational behavior. Before use, the F-EMS dataset underwent preprocessing to ensure measurement consistency. Sensor offsets were corrected using routine calibration logs, missing data were interpolated over short durations, and outliers were filtered based on statistical deviation thresholds. Through this preprocessing, the dataset achieved the accuracy required for quantitative energy balance calculations.

2.2. Energy balance analysis for the Paper drying process

In the paper-drying process, steam is supplied to drying cylinders, and the paper web passes over the heated cylinder surfaces, where moisture is evaporated by direct heat transfer. As evaporation proceeds, humid air accumulates inside the dryer hood, requiring a continuous supply of dry air and exhaust of moisture-laden air to maintain stable drying conditions. In the existing plant operation, residual steam after heat release in the drying process is condensed into low-temperature hot water and reused for utility purposes such as kitchen and shower hot water supply. Between the drying sections, a sizing process is applied to modify paper surface properties, after which the paper undergoes additional drying.

Based on this process, the energy balance was formulated by separating the system into three interacting components: steam, air, and paper. Steam-side heat input was determined from the enthalpy decrease between the inlet and outlet of the steam supplied to the drying cylinders using F-EMS measurements. On the air side, temperature and humidity data before and after the hood were used to evaluate the enthalpy increase of the process air, while air infiltration into the hood caused by pressure differences between the hood interior and the ambient environment was accounted for through mass balance calculations based on measured air flow rates.

The paper-side energy demand was represented by the drying load, calculated from the paper mass flow rate and moisture content at the inlet and outlet of the drying sections. The results showed that most of the supplied steam energy was consumed by moisture evaporation from the paper, while the remaining heat was discharged with the exhaust air. Heat loss through the hood wall and duct structure was neglected, as its contribution was minor compared with the total steam-side thermal input. Figure 3 illustrates the corresponding energy flow among the steam, air, and paper components.

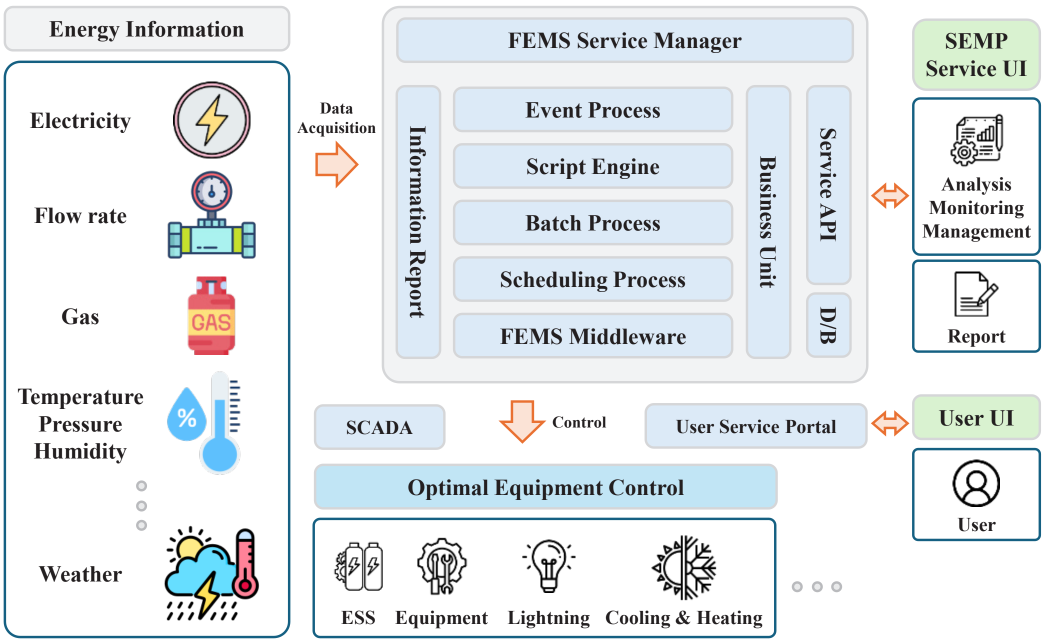

Figure 1. Configuration of Factory Energy Management System.

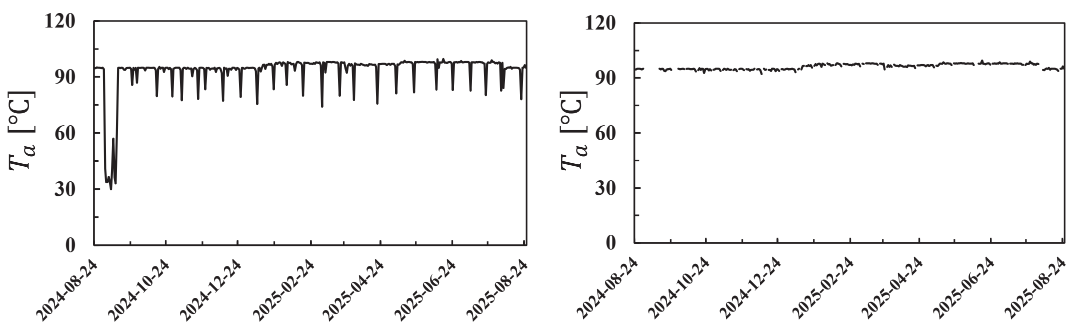

Figure 2. Pre-processing of long-term operational temperature data obtained from the F-EMS: (a) raw time series showing short-term disturbances and abnormal low-value intervals, (b) refined dataset after removal of non-representative operating periods and extraction of representative steady-state conditions.

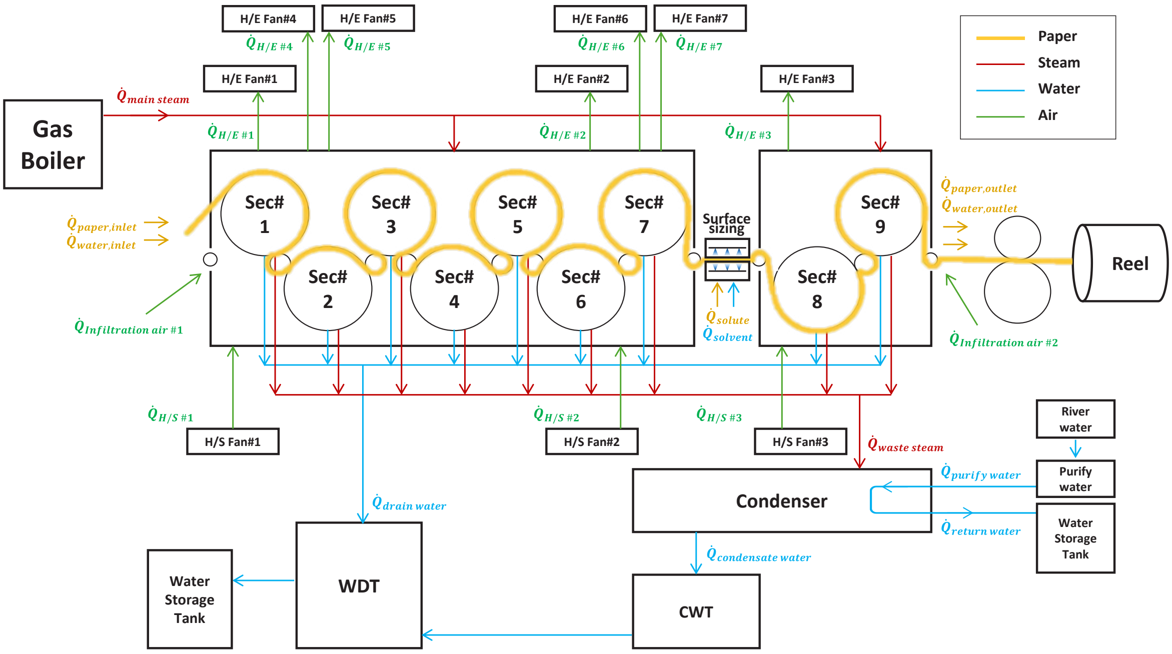

Figure 3. Paper drying process energy flow schematic.

3. Waste heat utilization

The waste heat analysis based on the F-EMS data revealed that a significant portion of the total energy loss in the paper-drying process originated from the pre-dryer hood exhaust streams. Even after moisture removal, these exhaust flows maintained relatively high temperatures and steady flow rates during continuous operation, making them the most promising sources for thermal recovery. The exhaust air temperature profiles obtained from the F-EMS remained consistent across different grades and production speeds, indicating that heat recovery could be achieved under stable operating conditions. To utilize this waste heat effectively, the study considered two thermal recovery methods suitable for industrial steam generation: a steam-generation heat pump (SGHP) and mechanical vapor recompression (MVR). The SGHP was applied to the air-side exhaust, whereas the MVR targeted the vapor-side condensate streams from the dryer section. These two systems were designed to be complementary: SGHP recovering low-grade exhaust heat, and MVR reusing process vapor directly from the dryer.

3.1. Steam generation heat pump (SGHP)

The SGHP is a thermodynamic system that converts low-grade heat from exhaust air into usable high-temperature steam through a closed vapor-compression cycle. The evaporator recovers heat from multiple pre-dryer exhaust ducts characterized in the F-EMS dataset, while the condenser supplies saturated or slightly superheated steam to the factory’s existing steam line. Because each exhaust stream has a different temperature and mass flow, the heat pump operation was evaluated by varying the air-side approach temperature (ΔT) between the exhaust air and the refrigerant evaporating temperature.

In this study, the SGHP was evaluated using a steady-state cycle model developed in MATLAB, and refrigerant thermophysical properties were calculated using REFPROP 10.0. The cycle model is not based solely on thermodynamic state points but also imposes practical heat-exchange feasibility by specifying pinch point temperature difference (PPTD) at the evaporator and condenser. The compressor was modeled with a fixed isentropic efficiency, and the discharge state was constrained to maintain a minimum superheat margin to avoid two-phase compression. The expansion process was assumed to be isenthalpic. R1233zd(E) was selected as the working fluid for this system [12-14]. It offers high thermal stability, low toxicity, and excellent two-phase heat-transfer characteristics at temperatures above 130 °C. Moreover, its low global warming potential (GWP=1) and zero ozone depletion potential (ODP=0) make it suitable for high-temperature industrial applications that require environmental compliance and long-term reliability. For each exhaust stream, steady-state calculations were performed using the measured boundary conditions to determine the corresponding steam generation rate, compressor power, and system COP. By scanning ΔT across a practical range, an optimum point ΔT^* was identified where the cost per unit steam was minimized. The resulting ΔT^*

values ranged between 15 °Cand 25 °C, depending on the local exhaust conditions. The SGHP performance was then aggregated for all seven exhaust streams, giving a total heat recovery rate consistent with the values obtained from the energy balance analysis.

3.2. Mechanical vapor recompression (MVR)

The MVR system compresses the low-pressure vapor released from the dryer section to a higher pressure so that it can be reused within the factory's steam network. It was considered as a complementary system to the SGHP, operating primarily on the process-vapor side. While the SGHP handles air streams with temperatures typically below 100 °C, the MVR upgrades saturated vapor from the dryer condensate line to a usable steam pressure. The compression ratio and discharge temperature were determined according to the steam conditions recorded in the F-EMS, allowing a fair comparison of performance and power demand between both systems.

In the model, the MVR compressor was represented using a fixed isentropic efficiency, and the discharge condition was constrained by a minimum superheat margin to prevent wet compression. For each target pressure level, the compressor work and discharge state were calculated from the inlet steam state and the required pressure lift. This modeling approach clarifies that the MVR evaluation is based on compressor thermodynamics (with operational constraints), rather than a purely conceptual representation. Simulation results indicated that when integrated properly, the MVR can supply a portion of the medium-pressure steam demand with relatively low electrical consumption, whereas the SGHP contributes more effectively to low-pressure steam generation. Therefore, an integrated configuration combining both technologies can cover a wider range of process steam requirements with higher overall efficiency.

3.3. System application scenarios

In the paper-drying process, exhaust air is discharged from multiple dryer sections along the production line. Each exhaust stream exhibits different temperature levels and flow characteristics depending on local drying conditions and ventilation requirements. Accordingly, the available waste heat is spatially distributed within the process rather than concentrated at a single location.

In this study, the recovered waste heat from each exhaust stream was evaluated individually in order to reflect these local characteristics and to identify suitable operating conditions for steam generation. This approach enables the heat pump operation to be aligned with the temperature level and availability of each heat source, providing flexibility in system operation under varying process conditions. Based on this integration concept, two application scenarios were investigated to evaluate how the recovered steam from the SGHP and MVR systems could be supplied to the existing steam network of the paper mill.

- *Scenario 1: Direct supply to the main steam header*
  In this configuration, the SGHP delivers steam at the same pressure level as the main header. The generated steam directly substitutes a portion of the boiler output. Because it must reach the highest pressure in the system, the compressor operates with a greater pressure ratio, leading to higher electrical consumption but also higher thermal flexibility. The model analysis based on F-EMS data showed that under low steam-demand conditions, this configuration achieves significant energy savings and can reduce annual operating costs by replacing part of the boiler load.

- *Scenario 2: Supply to the intermediate-pressure line*
  In the second configuration, the SGHP and MVR operate cooperatively. The SGHP first supplies steam to the intermediate-pressure line, meeting the low-pressure process demand, while the MVR upgrades the remaining vapor to a higher pressure when required. This approach reduces the overall power demand of the compressors and enhances the system COP compared to Scenario 1. Under the boundary conditions extracted from the F-EMS, the combined SGHP-MVR system achieved better economic performance, with annual cost savings exceeding those of the single-header configuration.

Both scenarios were evaluated using the measured exhaust-heat profiles and steam-demand data derived from the F-EMS. The comparative analysis demonstrated that integrating the SGHP at the intermediate-pressure level provides a more balanced operation between energy efficiency and electricity consumption, making it the preferred option for industrial implementation. Fig. 4 illustrates the conceptual integration of the SGHP and MVR systems with the existing steam network in the paper-drying process.

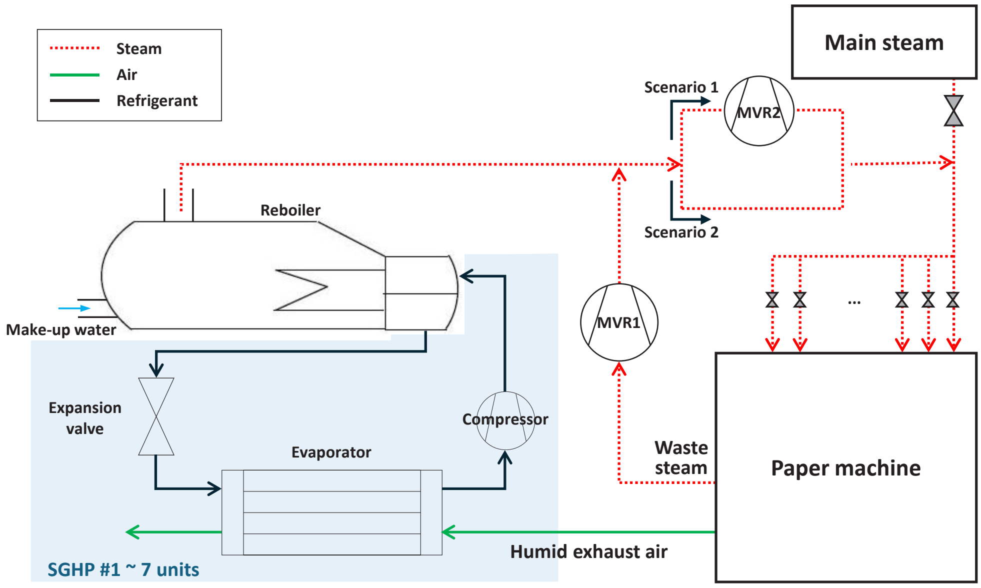

Figure 4. Schematic diagram of HTHP application for paper drying process.

4. Results and Discussion

The performance of the steam-generation heat pump (SGHP) was evaluated using the exhaust-air and steam-demand data collected from the factory energy management system (F-EMS). Based on the measured operating conditions, the thermodynamic cycle was modeled to determine the effect of the evaporator air-side temperature difference ($\Delta T_{evap,air}$) on the steam generation rate, compressor power, and coefficient of performance (COP). Fig 5 illustrates the simulation results for all seven exhaust streams. As shown in Fig. 5(a), the steam mass flow rate increases almost linearly with the air-side temperature difference, indicating that higher temperature lifts in the evaporator -enhance the heat recovery potential. However, as displayed in Fig. 5(b), this improvement is accompanied by a nonlinear increase in compressor work, particularly above $\Delta T_{evap,air} > 25$ °C. Consequently, the overall COP decreases with increasing ΔT, as shown in Fig. 5(c). The decline is primarily due to the higher compression ratio and greater discharge temperature associated with larger temperature lifts. To identify the most economical operating point for each exhaust stream, a cost-based optimization was performed. The optimum ΔT* corresponds to the condition where the cost of generated steam becomes minimal, balancing heat recovery and power consumption. Table 1 summarizes the optimal operating points for all seven exhaust streams. The optimal ΔT* values ranged between 15 °C and 25 °C, yielding COP values from 2.35 to 2.60. The total steam generation rate across all SGHP units reached 1.34 kg/s, while the combined compressor power was approximately 1.26 MW. These results were consistent with the energy balance findings described in Section 2, confirming that the modeled SGHP can effectively recover low-grade exhaust heat under realistic boundary conditions.

This study focuses on operating-cost-based (OPEX) evaluation to assess the relative performance of different integration strategies under identical boundary conditions. Investment cost estimation was not included, as capital expenditure strongly depends on site-specific factors such as equipment layout, degree of integration with existing infrastructure, and procurement conditions. By isolating OPEX, the present analysis highlights the thermodynamic and operational advantages of the proposed system configurations without introducing additional uncertainty associated with plant-specific cost assumptions. The economic performance of the SGHP was further compared with conventional heating methods. Fig 6 presents the cost comparison among a gas boiler, an electric heater, and the proposed heat pump system. The heat pump achieves the lowest operating cost in the ΔT range of 15-25 °C, corresponding to the region where the system operates near its optimal COP. The cost-saving potential relative to the gas boiler reached its maximum of approximately 0.06 MUSD/year at ΔT = 19 °C for SGHP #1, which was defined as the representative design point for subsequent analysis.

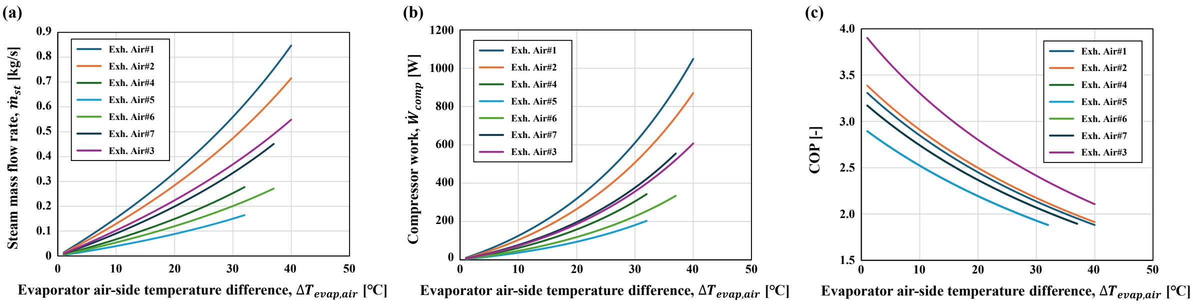

Figure 5. Variation of (a) steam mass flow rate, (b) compressor work, and (c) coefficient of performance (COP) for exhaust air #1-7 as a function of evaporator air-side temperature difference ($\Delta T_{evap,air}$).

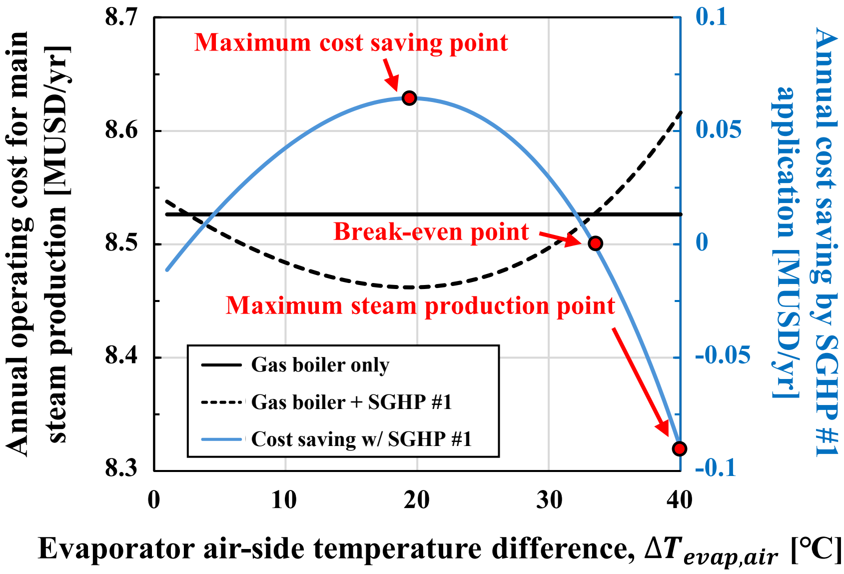

Figure 6. Annual operating cost and cost saving of SGHP #1 compared with boiler-only operation.

Table 1. Cost-optimal operating points for Exhaust Air #1-7

SGHP	ΔT*	COP_{SGHP}	W_{comp} (kW)	Steam flow rate (kg/s)
#1	19	2.49	295.6	0.315
#2	20	2.50	265.3	0.284
#3	25	2.60	263.1	0.293
#4	15	2.35	105.2	0.106
#5	15	2.35	62.3	0.063
#6	18	2.43	101.3	0.106
#7	18	2.43	168.2	0.176

After determining the optimal operating conditions of the individual SGHP units, the system was integrated into the plant's steam network to evaluate its overall performance. Two configurations were analyzed:

(1) Scenario 1, where the SGHP directly supplies high-pressure steam (8.2 bar, ≈170 ℃) to the main header, and
(2) Scenario 2, where the SGHP delivers medium-pressure steam (1.1-1.5 bar) to an intermediate line while the MVR recompresses the excess vapor as needed.

Fig. 7 compares the annual operating costs of the baseline boiler system and the SGHP-MVR configurations. In Scenario 1, the total power consumption reached 1.72 MW (1.26 MW for SGHP and 0.46 MW for the dual-stage MVR). The annual operating cost decreased from 8.53 MUSD to 8.15 MUSD, corresponding to a net saving of 0.38 MUSD. This direct integration provides operational flexibility for high-pressure steam use, but the additional compression required at 8.2 bar limits further improvement in efficiency. Scenario 2 demonstrated superior performance, as summarized in Table 2. When the integration pressure was gradually reduced from 1.5 to 1.1 bar, both the steam flow and system COP increased consistently, leading to larger cost reductions. At 1.5 bar, the combined system achieved a COP of 2.76 and displaced 2.51 kg/s of steam, resulting in an annual saving of 1.24 MUSD. At 1.1 bar, the COP improved to 2.91 with 2.82 kg/s of steam, yielding the maximum annual saving of 1.47 MUSD.

Although a lower integration pressure corresponds to a lower steam saturation temperature, the increase in steam mass flow rate observed at lower pressure levels is attributed to enhanced waste-heat recovery on the evaporator side. As the required condensation temperature decreases, the exhaust air can be cooled to a lower temperature, which expands the recoverable heat from the exhaust streams. As a result, the increase in total recovered heat outweighs the reduction in latent heat per unit mass, leading to an overall increase in steam generation rate at lower integration pressures. These results are further illustrated in Fig 8, which plots the total steam supply against annual cost savings for both scenarios. The direct integration (Scenario 1) is located at the lower left of the curve, showing moderate performance improvement over the baseline. In contrast, Scenario 2 shows a clear upward trend as the operating pressure decreases, confirming that a lower integration pressure enhances heat-pump efficiency and overall system economics.

From these findings, the intermediate-pressure integration strategy in Scenario 2 provides a more practical balance between efficiency and operating cost. It allows the SGHP to fully utilize the available exhaust heat while minimizing the required compressor power, ultimately improving the thermal performance and reducing the boiler load of the drying process.

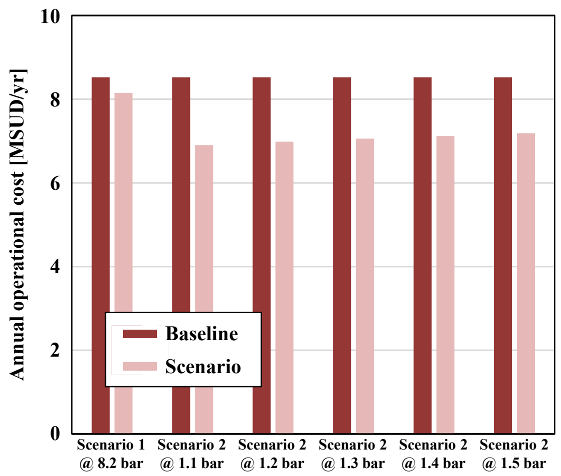

Figure 7. Operating cost of baseline and SGHP-MVR integration system

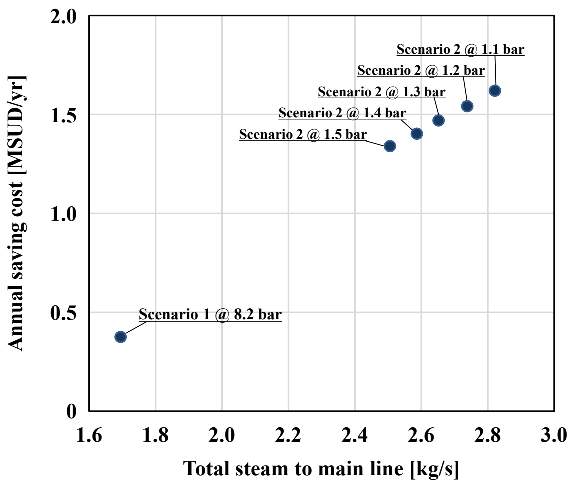

Figure 8. Annual cost saving according to total steam flow rate for scenario 1 and 2

Table 2. Cost-optimal operating points for Exhaust Air #1-7

Pressure (bar)	T_{sat} (°C)	Steam flow rate (kg/s)	COP_{sys}	Annual saving cost (MUSD/yr)
1.1	102	2.82	2.91	1.47
1.2	105	2.74	2.87	1.40
1.3	107	2.65	2.83	1.35
1.4	109	2.59	2.79	1.30
1.5	111	2.51	2.76	1.24

The obtained performance trends and operating ranges are in line with previously reported steam-generation heat pump (SGHP) and MVR applications, while the present study extends the discussion to process-scale integration based on plant operating data. For example, Koundinya et al. [15] reported a 60 kW-class SGHP producing 81.43 kg/h of steam at 108.5 °C and 1.5 bar using R245fa under a 50 °C waste-heat source, demonstrating feasibility of low-pressure steam generation from low-grade heat. Under comparable low-pressure steam levels (1.1-1.5 bar, Tsat = 102-111 °C), the present study evaluates an industrial paper-drying process and quantifies steam supply on a substantially larger scale (2.51-2.82 kg/s) with system COP values of 2.76-2.91, reflecting the effect of distributed exhaust heat streams and continuous operation.

In addition, the role of staged compression observed in this work is consistent with MVR studies. Bantle et al. [16] showed that two-stage MVR using turbo compressors can upgrade steam from near-atmospheric conditions to above 2.8 bar, enabling condensation around 131 °C, indicating that multistage compression is an effective approach when higher pressure levels are required. Similarly, the ANNEX58 demonstration reported by Ohmia Industry [17] achieved 150 °C steam at 5 bar by integrating SGHP and MVR systems, confirming the practicality of hybrid configurations for high-temperature steam supply. In this context, the present results highlight a process-integration trade-off: direct supply to the main header (Scenario 1) increases the required compression level and power demand, whereas intermediate-pressure integration (Scenario 2) reduces compression duty and improves COP, while still delivering meaningful steam displacement in the existing steam network.

Overall, while many previous studies have focused on component-level performance or simplified heat sources, the present work complements the literature by linking SGHP-MVR operating characteristics to plant-measured boundary conditions (F-EMS), thereby providing a process-level basis for selecting steam integration pressure and operating strategy in industrial drying applications.

5. Conclusion

This study demonstrated the technical feasibility of recovering low-grade exhaust heat from the paper-drying process using a steam-generation heat pump (SGHP) combined with mechanical vapor recompression (MVR). Through data obtained from the factory energy management system (F-EMS), the heat balance of the drying section was quantified, and multiple exhaust streams were identified as stable heat sources for high-temperature steam production. The SGHP exhibited stable performance within the realistic operating range of the exhaust air. The optimum air-side temperature difference for each stream was found to be 15-25 ℃, resulting in a total steam generation rate of 1.34 kg/s with moderate power demand. These results confirmed that the heat pump can effectively utilize exhaust energy while maintaining efficient operation under industrial conditions. Comparative analysis of integration strategies showed that direct connection to the main steam header can reduce part of the boiler load but provides limited cost benefit due to the high compression ratio. In contrast, the intermediate-pressure configuration achieved higher system efficiency and larger economic gains, reaching an annual cost reduction of up to 1.47 MUSD at 1.1 bar. This configuration offered the best balance between heat recovery potential and compressor energy consumption. Overall, the proposed SGHP-MVR system provides a practical approach to replacing fossil-fuel-based steam production with electricity-driven heat recovery. The results suggest that electrified steam generation using low-GWP refrigerants such as R1233zd(E) can contribute significantly to industrial decarbonization, particularly in continuous drying and process heating applications.

Acknowledgements

This research was jointly supported by National Research Foundation of Korea (RS-2024-00394625) and by Korea Institute of Energy Technology Evaluation and Planning (KETEP) (RS-2019-KP002048, RS-2024-00423446, RS-2024-00508737) funded by Ministry of Climate, Energy and Environment (MCEE). This work was also supported by Institute of Information & Communications Technology Planning & Evaluation (IITP)-Information Technology Research Center (ITRC) (IITP-RS-2024-00436248, 50). Authors sincerely appreciate their support. This work was also supported by Korea Evaluation Institute of Industrial Technology (KEIT) through the Automotive Industry Technology Development Program(RS-2024-00448767) funded by the Ministry of Trade, Industry & Energy(MOTIE).

References

[1] EINSTEIN, Dan; WORRELL, Ernst; KHRUSHCH, Marta. Steam systems in industry: Energy use and energy efficiency improvement potentials. 2001.

[2] WALKER, Michael E.; LV, Zhen; MASANET, Eric. Industrial steam systems and the energy-water nexus. *Environmental science & technology*, 2013, 47.22: 13060-13067.

[3] TUMANOVSKII, A. G., et al. Review of the coal-fired, over-supercritical and ultra-supercritical steam power plants. *Thermal Engineering*, 2017, 64.2: 83-96.

[4] ROMDHANA, Hedi; BONAZZI, Catherine; ESTEBAN-DECLOUX, Martine. Superheated steam drying: An overview of pilot and industrial dryers with a focus on energy efficiency. *Drying Technology*, 2015, 33.10: 1255-1274.

[5] ZHANG, Huang, et al. Superheated steam technology: Recent developments and applications in food industries. *Comprehensive reviews in food science and food safety*, 2024, 23.6: e70073.

[6] BADE, Mukund Haribhau; JANGAM, Sachin Vinayak; MUJUMDAR, Arun S. *Superheated Steam Drying: Technology for Improved Sustainability and Quality*. CRC Press, 2024.
[7] KLUTE, Sven, et al. Steam generating heat pumps–Overview, classification, economics, and basic modeling principles. *Energy Conversion and Management*, 2024, 299: 117882.
[8] van Deventer, H. C., Industrial Superheated Steam Drying, TNO-report, R 2004/239(2004).
[9] YANG, Han; YANG, Chunxin; GENG, Leiming. A heat pump-driven mechanical vapor compression desalination system and its operating characteristics. *Water Resources and Industry*, 2024, 32: 100264.
[10] ALI, Dalia Mohammed Talat Ebrahim; MOTUZIENĖ, Violeta; DŽIUGAITĖ-TUMĖNIENĖ, Rasa. Ai-driven innovations in building energy management systems: A review of potential applications and energy savings. *Energies*, 2024, 17.17: 4277.
[11] MOON, Yeeun, et al. Long short-term memory autoencoder and extreme gradient boosting-based factory energy management framework for power consumption forecasting. *Energies*, 2024, 17.15: 3666.
[12] WU, Di; WEI, Junzhuo; HU, Bin. Theoretical analysis, experimental research and industrial verification of high temperature heat pump based on R1233zd (E). *Energy*, 2025, 319: 135175.
[13] FENG, Ye. Comparative experimental investigations of evaporation heat transfer characteristics of R245fa and R1233zd (E) in an enhanced channel. *International Communications in Heat and Mass Transfer*, 2024, 152: 107261.
[14] JEẞBERGER, Jaromir, et al. Experimental investigations of upscaling effects of high-temperature heat pumps with R1233zd (E). *International Journal of Refrigeration*, 2024, 164: 243-256.
[15] Koundinya, Sandeep, J. Jothilingam, and Satyanarayanan Seshadri. Low-pressure steam generating heat pump–A design and field implementation case study. Thermal Science and Engineering Progress, 2023, 45: 102140.
[16] M. Bantle, C. Schlemminger, I. Tolstorebrov, M. Ahrens, K. Evenmo. Performance evaluation of two stage mechanical vapour recompression with turbo-compressors Proc. 13th IIR Gustav Lorentzen Conf. Nat. Refrig. (2018), p. 1157. 10.18462/iir.gl.2018.1157.
[17] [Online]. Available: https://heatpumpingtechnologies.org/annex58/wp-content/uploads/sites/70/2022/07/hthpannex58ohmiaindustryfinal.pdf [accessed:Jan. 12, 2023].